Submitted to Nuclear Physics

LBL-254
Preprint c.2

RECEIVED
LAWRENCE
RADIATION LABORATORY

LIBRARY AND
DOCUMENTS SECTION

INTERPRETATION OF MASS ASYMMETRY IN FISSION BASED ON DEFORMATION ENERGY SURFACES

C. F. Tsang and J. B. Wilhelmy

November 1971

AEC Contract No. W-7405-eng-48

TWO-WEEK LOAN COPY

This is a Library Circulating Copy which may be borrowed for two weeks. For a personal retention copy, call Tech. Info. Division, Ext. 5545

LAWRENCE BERKELEY LABORATORY
UNIVERSITY OF CALIFORNIA

LBL-254
c.2

34

DISCLAIMER

This document was prepared as an account of work sponsored by the United States Government. While this document is believed to contain correct information, neither the United States Government nor any agency thereof, nor the Regents of the University of California, nor any of their employees, makes any warranty, express or implied, or assumes any legal responsibility for the accuracy, completeness, or usefulness of any information, apparatus, product, or process disclosed, or represents that its use would not infringe privately owned rights. Reference herein to any specific commercial product, process, or service by its trade name, trademark, manufacturer, or otherwise, does not necessarily constitute or imply its endorsement, recommendation, or favoring by the United States Government or any agency thereof, or the Regents of the University of California. The views and opinions of authors expressed herein do not necessarily state or reflect those of the United States Government or any agency thereof or the Regents of the University of California.

INTERPRETATION OF MASS ASYMMETRY IN FISSION BASED ON DEFORMATION ENERGY SURFACES*

C. F. Tsang and J. B. Wilhelmy

Lawrence Berkeley Laboratory
University of California
Berkeley, California 94720

November 1971

Abstract

The deformation energy surfaces of fissioning nuclei have been studied to quantitatively interpret the experimentally observed mass asymmetry in fission. These studies use the calculated deformation energy surfaces which have recently been shown to have reflection asymmetric saddle point shapes in the second (outer) fission barriers of actinide nuclei. Quantitative estimates of the mass asymmetry in fission, characterized by the peak-to-valley mass yield ratio, have been calculated from an analysis of the fission probabilities over the outer barrier. The probability distributions were determined using the simple Fermi gas level density and the WKB barrier penetration formulae. Good correlations have been obtained for all known radiochemically determined peak-to-valley ratios of even-even fissioning nuclei for which deformation energy surface calculations are available. One is able to understand by this analysis the recently discovered apparently anamolous results that the thermal neutron induced fission of ^{257}Fm yields a symmetric mass division while the spontaneous fission of ^{256}Fm is fission asymmetric. A possible explanation for the triple-peaked mass yield fission

*Work performed under the auspices of the U. S. Atomic Energy Commission.

of nuclei near ^{226}Ra is proposed based also on the deformation energy surfaces. Further experiments are suggested to test the present theory, in particular, to discriminate between analyses based on the fission barrier in the deformation energy surfaces and those based on fragment shell effects.

Introduction

One of the most readily observed experimental properties of the fission process has been the determination of the mass distribution of the resultant fission products[1]). Shortly after the discovery of fission over thirty years ago it was determined that low energy neutron-induced fission yielded a distribution of fission products which were predominantly the result of an asymmetric mass division of the fissioning nucleus. Over the years many additional experimental studies have been performed to determine mass yield distributions of low energy induced fission. Until very recently the results of these studies have invariably shown the mass distribution to be strongly asymmetric. A typical mass yield distribution is shown in fig. 1. A characteristic measurement of the asymmetry is the ratio of the yield of fission products corresponding to the peak of the mass distribution to the yield of products at the valley. This peak-to-valley ratio has been explicitly determined in the case of the spontaneous fission of ^{252}Cf to be as large as $\sim$ 750, and for some other spontaneously fissioning nuclei only lower limits of this ratio have been found[3]). For all nuclei studied it has been found that as the fission-inducing excitation energy is increased, the peak-to-valley ratio decreases and eventually the distribution becomes symmetric about $A_o/2$. In all previous studies symmetric division does not occur until some 20-40 MeV of excitation energy is brought into the system. However, very recently an apparently anomalous case has been discovered in which the thermal neutron-induced fission of ^{257}Fm has resulted in a strongly symmetric mass distribution[4]). These results are even more striking because other current experimental studies have shown that the mass distribution for the spontaneous fission of the adjacent even-even isotope ^{256}Fm is asymmetric[5]).

Though many attempts have been made to theoretically interpret the fission mass distribution, none have been successful for quantitative predictions. The liquid-drop model analysis[6]) of the system predicts the mass distribution to be symmetric in all cases. Very often the asymmetry has been qualitatively explained as the result of strong shell effects in the residual fission product nuclei. These theories imply that the mass distribution is determined near the scission point since this is the region where the shell effects of the fragments dominate. Recently a more tractable theoretical interpretation of the mass distribution was proposed by Möller and Nilsson[7]) in which they have shown that in the actinide region, the second fission barrier has a lower total energy for asymmetric mass division. This is the first microscopic calculation which has shown a preference for asymmetric shapes in the fissioning nucleus. Since then, other groups, notably Nix et al.[8]), and Brack et al.[9]) have done somewhat more refined calculations with similar results. The Möller-Nilsson picture gives us a qualitative understanding of the mass asymmetry but no quantitative interpretation was attempted because of the belief that the difficult-to-calculate dynamical properties of the division would become important in determining the specific division.

In this paper we present a quantitative interpretation of the experimental fission-product mass yields based only on the calculated properties of deformation energy surfaces, without attempting a microscopic dynamic calculation. To do this we have used a very simple quasi-static theory to correlate all the known radiochemical data. We do not use mass determinations made from electronic measurements since the dispersion introduced by these

techniques partially fill the symmetric valley. For example, the peak-to-valley ratio of the mass yield curve derived for the spontaneous fission of ^{252}Cf may be off by a factor of 100 due to electronic dispersion effects[10]).

Specifically, we will try to relate the peak-to-valley ratio of the fission mass distribution to the saddle points of the deformation energy surface. Certainly the complete fission process involves not only the properties of the deformation energy surface near the saddle point, but also the shell effect of the final fission fragments as well as the dynamical path from the saddle to the scission point. What we are attempting to do in this paper is to look at one particular aspect of the problem quantitatively and to show how the peak-to-valley ratios can be understood on this basis. Other details of the mass yield curve, such as the widths of the distribution, may depend more strongly on the other aspects. A complete and quantitative study of the fission process involving all three aspects will lead to a better understanding of fission asymmetry.

It should be emphasized that our analysis does not employ the "two mode" hypothesis[11]). We use only one potential energy surface for a given nucleus. The probability of symmetric and asymmetric fission is based solely, in our simple picture, on the available excitation energy in the system as a function of deformation.

In the next section we will give a general discussion of our picture of the asymmetric fission process. One point that will come out is, that in our analysis, the asymmetric fission process is associated only with a localized region of large deformations near the second peak of the fission barrier. Hence, our study is concerned with properties of nuclei at very large deformations.

In the following three sections we will discuss in detail three possible cases of asymmetric fission depending on the excitation energy. After these, we will consider the mass yield curve of proton-induced fission of radium, which is one of the critical tests of any theory explaining fission asymmetry. A summary and suggestions for further experiments to test the theory will conclude this paper.

General Considerations

A deformation energy surface is a surface in a deformation-coordinate space that specifies the lowest total energy of a nucleus with a given deformation. It is calculated by combining the total energy given by the liquid-drop model analysis with shell corrections derived from single-particle spectra using the Strutinsky Prescription[9,17,12]. In the Möller-Nilsson calculation symmetric deformations described by the Legendre Polynomials $P_2(\cos\theta)$ and $P_4(\cos\theta)$ are considered as well as asymmetric deformations described by $P_3(\cos\theta)$ and $P_5(\cos\theta)$. A deformation given by $P_1(\cos\theta)$ corresponds only to a shift of the center of mass of the whole nucleus. In the calculations by Nix et al.[8], and Brack et al.[9] symmetric and asymmetric deformations are included in better sets of deformation coordinates which are able to describe very deformed shapes more adequately. In our analysis, we shall primarily employ the deformation energy surfaces calculated by Möller and Nilsson. Results obtained using those calculated by Nix et al. and Brack et al. will also be presented for comparison.

A typical deformation energy surface is sketched in fig. 2. The multidimensional aspects of the surface are reduced by combining the two symmetric coordinates (ε_2 and ε_4) and the two asymmetric coordinates (ε_3 and ε_5). The surface shows that the ground state, first fission barrier, and secondary minimum have their lowest energy along the symmetric axis (labelled SYM). However, the calculations show that the saddle point corresponding to the second fission barrier is located at an asymmetric deformation. Also shown in fig. 2 are cross sections of the deformation energy surface through the symmetric and asymmetric (labelled ASYM) axes. The cross section through the symmetric axis shows the

now familiar double-peaked fission barrier and that through the asymmetric axis shows that the deformation energy surface clearly prefers an asymmetric deformation.

This asymmetric saddle point indicates that at the outer barrier the fissioning nucleus prefers a nonsymmetric shape. The simplest picture of the fission process based on the deformation energy surface is one in which the nuclear deformation follows an adiabatic path of lowest energies from the ground state minimum to scission. To obtain symmetric fission, the path is restricted to the symmetric axis and it passes over the first peak, then the (isomeric) secondary minimum and over the (symmetric) mountain top to fission. When the restriction to the symmetric axis is relaxed the path will still follow the first peak and the secondary minimum along the symmetric axis as before. But from the secondary minimum, the path will deviate from the symmetric axis and seek to climb over the asymmetric saddle point to asymmetric fission. In the mass yield curve (fig. 1) the value at the valley corresponds to symmetric fission while the most probable yield occurs at an asymmetric mass divisions which corresponds to fission over the asymmetric saddle point. Hence the peak-to-valley ratio is a comparison of the two paths of fission. The portion of path from the ground state minimum, over the first barrier to the secondary minimum, that is common to both fission paths will be cancelled out in the peak-to-valley ratio and what needs to be studied is the difference in paths after the secondary minimum. Thus in our analysis of peak-to-valley ratios, we are concerned with properties of a nucleus at very large deformations. The nuclear shape at the secondary minimum has a ratio of axes approximately 1:2 and the shape at the symmetric mountain

top has a ratio of axes of approximately 1:2.7. At these large deformations, the relevant deformation points are the asymmetric saddle point and the symmetric mountain top. These are the equilibrium points in the deformation energy surface which are invariant under coordinate transformation, whereas non-equilibrium points have little physical meaning. We shall make use only of these points in the calculated deformation energy surfaces in our attempt to quantitatively interpret the peak-to-valley ratios experimentally observed in the fission process.

The deformation energy surface as a function of asymmetry at the second fission barrier lends itself to classification into three different cases to be considered in the fission process. These cases are shown in fig. 3 and are dependent on the excitation energy brought into the fissioning nucleus. Case I represents the situation when the excitation energy brought into the system is above both the symmetric and asymmetric fission barriers. Case II is when the energy is above the asymmetric barrier but below the symmetric barrier. Case III is when the energy is below both barriers. We will divide all of the experimental data into their appropriate cases and attempt to quantitatively interpret the observed peak-to-valley ratios.

Case I: Energy Above Both Barriers

For this case we propose that the probabilities of fissioning into symmetric and asymmetric products are proportional to the number of levels available at the symmetric and asymmetric barriers. To evaluate the number of levels for each case we use the simple Fermi-gas, level-density formalism

$$P_s = ce^{2\sqrt{a(E_T-E_s)}}$$

$$P_a = ce^{2\sqrt{a'(E_T-E_a)}} \quad ,$$

where P_s and P_a are the probability for symmetric and asymmetric division respectively; E_T is the excitation energy; E_s and E_a are the energies of the symmetric and asymmetric barriers; and a and a' are the level density parameters for the symmetric and asymmetric cases respectively. The height of the symmetric barrier above the asymmetric barrier is designated h, that is,

$$h = E_a - E_s \quad .$$

In the Fermi-gas model the level-density parameters are proportional to the number of particles (A) and can therefore be written as

$$a = \chi A$$

$$a' = \chi' A \quad .$$

Making these substitutions and taking the ratio of the probability of asymmetric to symmetric fission yields, we get

$$\ln \frac{P_a}{P_s} = 2\sqrt{\chi' A(E_T-E_a)} - 2\sqrt{\chi A(E_T-E_s)} \quad . \qquad (1)$$

It can be easily seen that this equation has the correct asymptotic properties. If h goes to zero (i.e. the difference between the symmetric and asymmetric barrier disappears), then χ and χ' become equal and the right-hand portion of the equation goes to zero; and, therefore, the probability ratio of asymmetric to symmetric fission goes to one. When E_T (the excitation energy) becomes very large relative to h, χ and χ' become equal and the right-hand side of the equation again becomes zero, which again predicts symmetric fission.

Equation (1) may be written as

$$1 = 2\sqrt{\chi'}\ \frac{\sqrt{A(E_T-E_a)}}{\ln \frac{P_a}{P_s}} - 2\sqrt{\chi}\ \frac{\sqrt{A(E_T-E_s)}}{\ln \frac{P_a}{P_s}} \quad . \tag{2}$$

A plot of $\sqrt{A(E_T-E_a)}\Big/\ln\,(P_a/P_s)$ against $\sqrt{A(E_T-E_s)}\Big/\ln\,(P_a/P_s)$ should be linear if χ and χ' are constant. To make such a plot, it is necessary to evaluate the various quantities in the ordinate and abscissa. The ratio of probabilities, P_a/P_s, of asymmetric to symmetric fission is taken to be the experimentally observed[3]) peak-to-valley ratio (p/v):

$$\frac{P_a}{P_s} = \frac{p}{v} \quad .$$

The excitation energy E_T is given for neutron-induced fission by the sum of the kinetic energy of the incident neutron and the experimental neutron binding energy of the compound nucleus. The energy of the asymmetric saddle point is identified as the empirical barrier height of the second (outer) fission barrier. These empirical values were derived from the analysis of experimental data by Bjørnholm[13]), Britt et al.[14]), and Back et al.[15]). In cases where empirical

values are not available we have used the semi-empirical values of Pauli and Ledergerber[16]), who also tabulated the values of $h = E_a - E_s$ from calculations based on the work of Brack et al.[9]). The values for E_s are obtained by adding the energy difference, h, between the asymmetric saddle and the symmetric mountain top to the height of the outer fission barrier, E_a. Thus h is the only number we get from the theory and in this way we hope to be free, as much as possible, from all the uncertainties of the theory.

Table 1 presents the values used in calculating the ordinate and abscissa for eq. (2) and fig. 4 presents a plot of these data based on the Möller-Nilsson deformation energy surfaces (using surface-dependent pairing strengths). The data at large excitation energies correspond to large values on the ordinate and abscissa. As can be seen, these data define a reasonable straight line, with some deviation at the low-energy end. The magnitudes of χ and χ' are determined from the line. They are found to be equal (which is reasonable, since for high energies, the effect of h is unimportant) and of the value 1/10. This gives for the level density parameter in the Fermi-gas model, $a = A/10$, which is in good agreement with the value obtained from an analysis of neutron-capture resonances and of other nuclear reactions where a is typically determined to be between A/8 to A/12. For low-energy points, both χ and χ' are seen to be no longer constant as a function of energy. Their values at any point may be determined from the tangent to a smooth curve passing through the data points. Since the smooth curve bends up from the straight line as one goes to decreasing values on the abscissa, this means the value of χ' is decreasing (the tangent intercept on the ordinate is a larger number) implying a decrease in the number of levels when the energy is close to the deformation energy surface.

Figure 5 displays the same plot for other calculations of deformation energy surfaces. Good correlations of all experimental data are obtained in all versions, and the various versions lie very close to each other. The values of χ determined from lines corresponding to the Nix and Pauli-Ledergerber calculations are smaller, $\chi \simeq 1/36$, which shows that the present analysis is not a sensitive method to obtain the value of the level density parameter. Small shifts of the lines will result in large changes in the value of χ.

To make predictions of the peak-to-valley ratio of thermal neutron-induced fission of ^{257}Fm, we modify eq. (2):

$$\frac{1}{\sqrt{A(E_T-E_s)}} \ln \frac{p}{v} = 2\sqrt{\chi'} \sqrt{\frac{E_T-E_a}{E_T-E_s}} - 2\sqrt{\chi} \quad ; \quad \frac{p}{v} = \frac{P_a}{P_s} \tag{3}$$

The plot of the left-hand side against $\sqrt{(E_T-E_a)/(E_T-E_s)}$ is shown in fig. 6 using Möller and Nilsson's deformation energy surfaces. From the calculated abscissa value for the thermal neutron induced fission of ^{257}Fm we predict its peak-to-valley ratio to be 1·8. This compares well with the experimental value of 1 (i.e. symmetric fission) since the range of values we are talking about is from 1 to about 750. The uncertainties in theory are more than enough to account for the difference of 1·8 from 1. The physical reason why we have close-to-symmetric fission in this case is that the energy difference, h, between asymmetric saddle point and the symmetric mountain top is small (only 0.2 MeV) so that at the neutron binding energy, 3.2 MeV above the barrier, its effect is not large. In other cases such as U and Pu, h is about 2 MeV and has a significant effect for excitation energies corresponding to thermal neutron fission.

When we carry out a similar calculation with Nix's or Pauli-Ledergerber's deformation energy surfaces, we obtain a much larger value of peak-to-valley ratio for the prediction: 3600 and 60, respectively. The main reason is that, Nix's and Pauli-Ledergerber's calculations give a very large value of h for ^{258}Fm (2.2 MeV and 1.9 MeV respectively). These very large values of h may be due to the fact that Nix and Pauli-Ledergerber do not use enough shells in the calculation basis for such large asymmetric deformations.† The inclusion of many shells may lower the value of h which would thus tend to make it consistent with the experimental results. At the moment we also have some reservations about the Nix value since this model also predicts a large value of h for Po where no asymmetric fission is observed.

†As a technical point, we would like to point out that it is <u>not</u> true that an increase in size of the basis will always bring down the total energy of the nucleus. What is decreased is the summation of energies of the occupied single-particle levels, but the shell correction can be either larger or smaller.

Case II; Intermediate

In this case the input energy is above the asymmetric barrier but below the symmetric barrier. The probability of asymmetric fission will still be taken as proportional to the number of levels available for the fission process.

$$P_a = ce^{2\sqrt{\chi' A(E_T - E_a)}}$$

where the symbols have the same meaning as in the previous case. For symmetric fission, however, the excitation energy is below the barrier, and therefore the probability for symmetric fission will be dependent on the probability that the barrier can be penetrated. The standard WKB barrier penetration formalism is used and yields the probability for symmetric fission to be

$$P_s = c' \left\{ \frac{1}{1 + \exp\left[2\int\sqrt{\frac{2\beta}{\hbar^2} A^{5/3} \left|E_s - E_T\right|}\, d\varepsilon\right]} \right\}$$

where $\beta A^{5/3}$ is the inertial parameter of the fissioning nucleus and the integral is evaluated over the penetration path.

For continuity with Case I, i.e. P_s should be the same in value whether the Fermi-gas level density formula or the penetrability formula is used for the case $E_T = E_s$, it is seen that

$$c' = 2c \quad .$$

It turns out that for the data available, it is a very good approximation to assume that the exponential term in the denominator of the expression for P_s to be large so that

$$P_s = c' e^{-2\int\sqrt{\frac{2\beta}{\hbar^2} A^{5/3}(E_s-E_T)}\, d\varepsilon} .$$

Using a parabolic approximation for the barrier shape to be penetrated we may write P_s in terms of a quantity $\hbar\omega$.

$$P_s = c' e^{-\frac{2\pi}{\hbar\omega}(E_s-E_T)} .$$

The quantity $\hbar\omega$ is sometimes known as the transparency and it is dependent on both the inertia parameter and the curvature of the barrier, and is proportional to $A^{-5/6}$ in the simple irrotational flow model.

As in case I, we take the ratio P_a/P_s and after a little algebra, we obtain

$$\frac{1}{A^{5/6}(E_s-E_T)} \ln \frac{2P_a}{P_s} = 2\sqrt{\chi'}\, \frac{\sqrt{E_T-E_a}}{A^{1/3}(E_s-E_T)} + \frac{2\pi}{\hbar\omega A^{5/6}} \qquad (4)$$

In the last term we have tried to take the A-dependence of $\hbar\omega$ out by multiplying it by $A^{5/6}$ so that it is a constant term if the inertia and curvature of barrier stay about the same.

In fig. 7 the left-hand side of the above equation is plotted against $A^{-1/3}\sqrt{E_T-E_a}/(E_s-E_T)$ based on Möller and Nilsson's deformation energy surfaces. The data are shown in Table 1. There are only four experimental

points that fall into this present case and they show very good correlation. The slope gives a value for $\chi' = \frac{1}{48}$. This is much smaller than the value obtained for high energies from Case I. One possible explanation is that at the asymmetric saddle point one is experiencing a shell effect in the Strutinsky sense[9]) relative to the symmetric mountain top, and a shell effect implies a low-level density. When one refers to the single-particle level diagrams calculated by Nilsson et al.[18,12]), and counts the levels in a given energy range about the Fermi level, it is found that at two deformations whose shell energy differs by 2 MeV, the single-particle level densities may differ by a factor of three. The ordinate-intercept of the plot gives for the transparency $\hbar\omega = 3.3$ MeV for $A = 238$. This number is much too large when compared with the usually accepted empirical values that range from 0.5 to 1.5 MeV. The reason is unclear. It may be due to zero-point-energy effects which are important in this present case because the excitation energy is within two MeV of the barrier. It may also be due to the very approximate but simple formulas that we have used for evaluating the fission probabilities.

For comparison with calculations based on deformation energy surfaces of Nix, and Pauli-Ledergerber, similar plots are shown in fig. 8. There are more experimental points falling into case II with Nix's and Pauli-Ledergerber's results. Each set of data still lie on very reasonable straight lines. The values of the transparency $\hbar\omega$ based on Nix's and Pauli-Ledergerber's results remain approximately the same. The value of χ is even smaller ($\chi \sim 1/100$).

Case III: Energy Below Both Barriers

In this case the energy is below both the symmetric mountain top and the asymmetric saddle. All the data we have found that fall into this category are obtained by spontaneous fission studies (i.e. $E_T = 0$). Both the probability of symmetric fission and the probability of asymmetric fission are given by the standard WKB formula

$$P_a = c' e^{-2\int \sqrt{\frac{2\beta'}{\hbar^2} A^{5/3} (E_a - E_T)}\, d\varepsilon}$$

$$P_s = c' e^{-2\int \sqrt{\frac{2\beta}{\hbar^2} A^{5/3} (E_s - E_T)}\, d\varepsilon}$$

where $\beta' A^{5/3}$ is the inertia parameter of penetrating through the asymmetric saddle, and $\beta A^{5/3}$ is that through the symmetric mountain top. On taking the ratio of probabilities, the penetration path from the ground state to the secondary minimum that is common to both cancel out, and we need only consider the penetration from the secondary minimum to the emerging point out of the barrier by way of the asymmetric saddle or the symmetric mountain top. We approximate the barrier shape for such penetration by a parabola that passes through the secondary minimum and the emerging point with the top of the parabola at the same energy as the asymmetric saddle (or the symmetric mountain top) (see fig. 9). The result is the following:

$$\ln \frac{P_a}{P_s} = \left\{ \sqrt{\frac{2\beta}{\hbar^2}} \sqrt{E_s}\, f(E_s - E_i,\ E_s) - \sqrt{\frac{2\beta'}{\hbar^2}} \sqrt{E_a}\, f(E_a - E_i,\ E_a) \right\} A^{5/6}\ d$$

where $$f(c,a) = \left\{ \sqrt{\frac{c}{a}\left(1 - \frac{c}{a}\right)} + \frac{\pi}{2} + \sin^{-1}\sqrt{\frac{c}{a}} \right\} \Big/ \left(1 + \frac{c}{a}\right) \qquad (5)$$

and d is the penetration path length from the secondary minimum to the emerging point and its values (assumed to be the same for both the symmetric and asymmetric fission paths) were obtained from barrier shapes calculated by Nilsson et al.[12]). E_i is the energy of the secondary minimum above the ground state, which we take from the empirical values of isomeric threshold energies (Table 1).

In this equation there are two parameters to be determined. Up until recently there has been only one radiochemical result of the peak-to-valley ratio for spontaneous fission, which is the case of ^{252}Cf ($p/v \approx 750$). The other spontaneous fission results are given only as lower limits. As a reasonable number we have taken an empirical value for β' from fitting spontaneous fission half-lives to the barrier shapes calculated by Nilsson et al.[12]). This value turns out to be given by

$$\sqrt{\frac{2\beta'}{\hbar^2}} = 0.3390 \text{ MeV}^{-1/2} \tag{6a}$$

with reference to Nilsson's deformation coordinates. Then the β value is obtained by fitting the ^{252}Cf peak-to-valley ratio as given by P_a/P_s in the above equation:

$$\sqrt{\frac{2\beta}{\hbar^2}} = 0.3747 \text{ MeV}^{-1/2} \tag{6b}$$

It is to be noted that β' is smaller than β but only slightly. It is reasonable that β' is smaller than β since the level density at the symmetric mountain top is larger than that at the asymmetric saddle, and theoretical calculations indicate that the inertial parameter should increase with increasing level density[9]). However, the finding that β and β' are approximately equal may

appear to be in contradiction with calculations that show that inertia parameters at the barriers and the minima may differ by a factor of three.

With the values of β and β' thus determined, the peak-to-valley ratios can be calculated. The results are tabulated in Table 2. Thus the mass yield of the spontaneous fission of ^{256}Fm is calculated to have peak-to-valley ratio of 43 which compares reasonably well with the experimental number of 12 [5]). The physical reason why the fission of ^{256}Fm is asymmetric is that even though the energy difference, h, between the asymmetric saddle and the symmetric mountain top is small, in the case of tunnelling under the barrier, it is felt quite strongly. This is to be contrasted with the case of the thermal neutron-induced fission of ^{257}Fm, where h is just as small, but its effect is very little when the excitation energy is substantially above the barrier. A critical test of the present theory will be to measure the peak-to-valley ratio of the thermal neutron induced fission of ^{255}Fm (which we predict to fission symmetrically) or of the spontaneous fission of ^{258}Fm (which we predict to fission asymmetrically).

The Radium Region

It is well-known that the mass yield curve of proton-induced fission of ^{226}Ra has three peaks[19,20]); that is to say, the probability of fission is large for both symmetric and asymmetric fission. In our picture this requires three minimum-energy paths across the outer barrier, one at the symmetric axis, one at an asymmetric configuration and the third at a shape corresponding to the mirror image of the asymmetric configuration. Möller and Nilsson[7]) recently calculated the deformation energy surface of a nearby nucleus ^{222}Ra, (in contrast to their previous calculations, they have used in this case a surface-independent pairing strength) which displays such a feature. Their results are shown in fig. 10. In the figure, beyond the secondary minimum, in the outer barrier region, one finds two mountains situated at some asymmetric deformation. Between the two mountains is the symmetric path which is energetically favorable. On further sides of the two mountains are the asymmetric paths which are also favored. Such a structure would produce a triple peaked mass yield curve for the fissioning nucleus. Similar calculations by Nix do not show this triple valley feature and therefore in our model cannot be used to interpret this particular experimental mass distribution. However, even the Möller-Nilsson picture is unable to account for the observation that at low energies, the asymmetric peaks of the mass yield curve are much higher than the symmetric peak but at high energies they are lower, and at some intermediate energy (~ 11 MeV bombarding energy in case of proton-induced fission of ^{226}Ra) the three peaks are about equal[20]). The failure of our picture to understand such a switching-over of the highest peak may be illustrated in fig. 11, which shows that as the excitation energy is increased,

the three peaks will smear out into a flat-top mass yield curve without the switch-over occurring at any energy.

One way to account for the switch-over is to realize that the shell effect can be a function of excitation energy. The energy of symmetric path above the asymmetric paths in the outer barrier is very small according to Möller and Nilsson. Actually in our estimation, to cause the peak-to-valley ratio of mass yields to be 2, one needs only an energy difference of about 0.2 MeV. It is perhaps not inconceivable that as the excitation energy is increased, the shell effects are altered such that the energy difference is changed from +0.2 MeV to -0.2 MeV, thus effecting a switch-over in the mass-yield peaks.

Another possible explanation may be that the switch-over is to a large extent due to the presence of a higher chance fission (i.e. the fission of the compound nucleus after one or more neutrons are evaporated). It has recently been found by Perry and Fairhall[21]) that the first chance fission of ^{228}Ac at 18 MeV excitation energy is symmetric. This is a surprising result since it has been long established that for a wide range of energies the fission yield of ^{227}Ac is triple-peaked. The sudden change to symmetric fission of the adjacent isotope is not understood as yet. It may be due to the fact that ^{228}Ac is an odd-odd nucleus. If ^{226}Ac, the adjacent odd-odd nucleus, is also fission symmetric, then we suggest that the proton-induced fission of ^{226}Ra is composed of the fission of ^{227}Ac and the second chance fission of ^{226}Ac:

$$\begin{array}{ccccc} p + {}^{226}\mathrm{Ra} & \longrightarrow & {}^{227}\mathrm{Ac} & \longrightarrow & {}^{226}\mathrm{Ac} + n \\ & & \downarrow & & \downarrow \\ & & \text{fission} & & \text{fission} \end{array}$$

At low excitation energies, only first chance fission is energetically possible, and one sees only ^{227}Ac fissioning and this gives generally a triple-peaked mass yield curve with asymmetric peaks much higher than the symmetric peak. As one increases the energy, the second chance fission (^{226}Ac) sets in and its symmetric mass yield is also present in the final mass yield measurement.

Using the liquid drop barriers of ^{227}Ac and ^{226}Ac as given by Myers and Swiatecki[22]), Gatti[23]) finds that the second chance fission sets in at about 10 MeV of bombarding energy and the second chance fission yield stays about constant [at 17-50% corresponding to the value of a_F/a_n, (the ratio of the Fermi level density parameter at the saddle and at the ground state) equal to 1.2 or 1.0 respectively] relative to the first chance fission until the third chance fission sets in at about 18 MeV proton bombarding energy. The effect of the second chance fission on the final mass yield is shown schematically in fig. 12. This figure shows the mass yield for the first chance fission (^{227}Ac), the second chance fission (^{226}Ac), and the cumulative mass yield (SUM) which is what is observed experimentally. These yields are shown at five proton bombarding energies (E_p). This shows a plausible explanation for the experimentally observed switch-over of the symmetry and asymmetry mass yield peaks at about E_p = 11 MeV.

Summary and Conclusion

In this study it is shown that a quantitative interpretation of all available peak-to-valley ratios in the fission mass yield curve can be obtained based on the deformation energy surface. Furthermore, some information concerning level density parameters and inertia parameters are obtained in the region around the second barrier. The analysis has been performed using three different sets of deformation energy surface calculations (Möller-Nilsson, Nix, and Pauli-Ledergerber). All three have been successful in predicting the general trends of the mass distribution as a function of the energetics of the fissioning nucleus. However, the results of Möller-Nilsson yield the best quantitative agreement with experiment. From the satisfactory correlations that come out of the present analysis, it may appear that before a good and realistic dynamic calculation is done on fission asymmetry, it is perhaps profitable to look at the problem from a quasi-static point of view with more sophisticated fission probability formulae than those employed in this paper.

The two most important physical quantities that affect the mass yield curve are first, the excitation energy above the outer barrier and secondly, the energy difference, h, between the symmetric mountain top and the asymmetric saddle. When h is zero or small, there is little difference between the symmetric fission path and asymmetric fission path, and the peak-to-valley ratio is expected to approach one. When h is large, of course, asymmetric fission prevails. The mass yield curve is also quite a strong function of the excitation energy. As the energy is well above the barrier, the effect of h is not seen and symmetric fission is observed. But as the energy is decreased, the effect of h becomes more significant and causes asymmetric fission.

In this picture it is possible to explain the recent data of the spontaneous fission of ^{256}Fm and the neutron-induced fission of ^{257}Fm. For the latter case, h is small, and even at the energy of thermal neutrons, one is sufficiently above the outer barrier not to feel too much the effect of h and hence the peak-to-valley ratio is close to unity. In the same way, our analysis would predict the fission of thermal neutron-induced fission of ^{255}Fm to be symmetric. For the case of the spontaneous fission of ^{256}Fm, even though h is small, the excitation energy is zero, i.e. the fission is a penetration process through the barrier, which can feel even the small value of h and thus asymmetric fission is observed. In the same way, our analysis would predict the spontaneous fission of ^{258}Fm to be asymmetric.

Experiments to measure mass yields of the spontaneous fission of ^{258}Fm and the thermal neutron-induced fission of ^{255}Fm would be strong tests of our theory. They will also help to differentiate between our theory which is based on a quasi-static analysis in the region of the second barrier and the theory often advocated that the fission asymmetry is due to fragment shell effects, determined predominantly near the scission point. In the later theory, the mass yield curve of spontaneous fission of ^{258}Fm (and of ^{256}Fm) would be very similar to the thermal neutron-induced fission of ^{257}Fm (and of ^{255}Fm).

Other very crucial experiments in the further understanding of fission asymmetry are those measuring the mass yield of nuclei in the radium region, in particular, the low energy fission yield of polonium isotopes. This region provides critical test of any theory of fission. Further experiments, especially those in which higher chance fission can be substracted will be extremely valuable.

Acknowledgments

We would like to acknowledge with appreciation the encouragments and advice of Dr. Stanley G. Thompson during the course of this work. Discussions with Drs. H. C. Britt, Eli Cheifetz, Walter John, W. D. Myers, J. R. Nix, H. W. Schmitt, W. J. Swiatecki, John Unik, and J. J. Wesolowski have been most helpful. We are also grateful to Drs. Peter Möller, S. G. Nilsson, J. R. Nix, H. C. Britt, and R. C. Gatti for supplying us with their calculations before publication.

References

1) E. K. Hyde, The Nuclear Properties of the Heavy Elements, III, Fission Phenomena, Prentice-Hall Inc., Englewood Cliffs, New Jersey (1964)

2) S. Katcoff, Nucleonics 18 (1960) 201

3) H. R. Von Gunten, Actinides Rev. 1 (1969) 275

4) W. John, E. K. Hulet, R. W. Lough, and J. J. Wesolowski, Phys. Rev. Letters 27 (1971) 45

5) K. F. Flynn, E. T. Horwitz, C. A. Bloomquist, R. F. Barnes, R. K. Sjoblom, and L. E. Glendenin, submitted to Physical Review

6) W. J. Swiatecki and S. Cohen, Ann. Phys. (N.Y.) 22 (1963) 406; J. R. Nix, Nucl. Phys. A130 (1969) 241

7) P. Möller and S. G. Nilsson, Phys. Letters 31B (1970) 283; also, private communications (1971)

8) J. R. Nix, private communications (1971); M. Boltsterli, E. O. Fiset, J. R. Nix, and J. L. Norton, submitted to Phys. Rev. C (Los Alamos Scientific Laboratory Report LA-DC-12817)

9) M. Brack, Jens Damgaard, H.-C. Pauli, A. Stenholm-Jensen, V. M. Strutinsky, and C. Y. Wong, "On Nuclear Shell Effects", to be published in Review of Modern Physics

10) R. Brandt, Lawrence Radiation Laboratory Report UCRL-10481 (1962)

11) A. Turkevich and J. B. Niday, Phys. Rev. 84 (1951) 52; J. B. Niday, Phys. Rev. 121 (1961) 1471; H. Baba and S. Baba, Nucl. Phys. A175, 199 (1971)

12) S. G. Nilsson, C. F. Tsang, A. Sobiczewski, Z. Szymanski, S. Wycech, C. Gustafson, I.-L. Lamm, P. Möller, and B. Nilsson, Nucl. Phys. A131 (1969) 1

13) S. Bjørnholm, in Proceeding of the Conference on Transuranium Elements--The Mendeleev Centennial (Robert A. Welch Foundation, Houston, 1969) p. 447

14) H. C. Britt, S. C. Burnett, B. H. Erkkila, J. E. Lynn, and W. E. Stein, Phys. Rev. C 4 (1971) 1444

15) B. B. Back, J. P. Bondorf, G. A. Otroschenko, J. Pederson, and B. Rasmussen, Nucl. Phys. A165 (1971) 449

16) H. C. Pauli and T. Ledergerber, to be published

17) V. M. Strutinsky, Nucl. Phys. A95 (1967) 420

18) S. G. Nilsson and P. Möller, private communications (1971)

19) R. C. Jensen and A. W. Fairhall, Phys. Rev. 109 (1958) 942

20) E. Konecny and H. W. Schmitt, Phys. Rev. 172 (1968) 172

21) D. G. Perry and A. W. Fairhall, Phys. Rev. C 4 (1971) 977

22) W. D. Myers and W. J. Swiatecki, Nucl. Phys. 81 (1966) 1; Lawrence Radiation Laboratory Report UCRL-11980

23) R. C. Gatti, private communication (1971)

Table 1. Quantities used in eq. (2-5) for determining peak-to-valley ratios.

Nucleus	P_a/P_s [a]	Incident neutron energy (MeV)	B_N [b] (MeV)	E_T [c] (MeV)	E_i [d] (MeV)	E_a [e] (MeV)	E_s [f] Nil-I[g] (case)	Nil-II[h] (case)	Pauli[i] (case)	Nix[j] (case)
^{234}U	390	0	6.9	6.9	2.7[k]	6.0[ℓ]	8.24(II)	9.1(II)	9.1(II)	8.5(II)
	120	2.5		9.4			(I)	(I)	(I)	(I)
	5	14.		20.9			(I)	(I)	(I)	(I)
^{236}U	600	0	6.6	6.6	2.4[m]	6.0[ℓ]	8.48(II)	9.3(II)	9.7(II)	9.4(II)
	150	2.5		9.1			(I)	(II)	(II)	(II)
	73	5.		11.6			(I)	(I)	(I)	(I)
	21	8.		14.6			(I)	(I)	(I)	(I)
	7	14.		20.6			(I)	(I)	(I)	(I)
^{238}U	>500	S.F.	6.8	0	2.0[k]	5.8[ℓ]	8.43(III)	9.1(III)	10.0(III)	9.9(III)
^{240}Pu	>270	S.F.	6.8	0	2.6[n]	5.4[n]	7.3 (III)	7.9(III)	9.1(III)	8.8(III)
	235	0		6.8			(II)	(II)	(II)	(II)
	~ 90	2.5		9.3			(I)	(I)	(I)	(I)
	6	14.		20.8			(I)	(I)	(I)	(I)
^{242}Pu	290	0	6.5	6.5	2.2[ℓ]	5.3[ℓ]	7.2 (II)	7.7(II)	9.0(II)	8.8(II)
^{242}Cm	>700	S.F.	6.9	0	3.2[n]	5.1[ℓ]	6.4 (III)	7.0(III)	8.1(III)	8.0(III)
^{244}Cm	$>5\times10^{3}$[(o)]	S.F.	6.7	0	2.6[k]	5.3[k]	6.6 (III)	7.0(III)	8.3(III)	8.2(III)

(continued)

Table 1 (continued)

Nucleus	P_a/P_s [a]	Incident neutron energy (MeV)	B_N [b] (MeV)	E_T [c] (MeV)	E_i [d] (MeV)	E_a [e] (MeV)	E_s [f] Nil-I[g] (case)	E_s [f] Nil-II[h] (case)	E_s [f] Pauli[i] (case)	E_s [f] Nix[j] (case)
^{246}Cm	140	0	6.6	6.6	3.1[k]	5.4[k]	6.6 (I)	7.0(II)	8.5(II)	8.0(II)
^{250}Cf	> 60	0	6.7	6.7	3.1[k]	4.5[k]	5.1 (I)	5.3(I)	7.3(II)	7.3(II)
^{252}Cf	~ 750	S.F.	6.0	0	2.7[k]	4.0[k]	4.5 (III)	4.4(III)	6.5(III)	6.5(III)
^{258}Fm	~ 12[(o)]	S.F.	6.8[p]	0	2.0[k]	3.4[k]	3.6[q](III)		5.3(III)	5.6(III)
^{258}Fm	Sym[r]	0	6.5[p]	6.5	2.0[k]	3.3[k]	3.5[q](III)		4.5(I)	5.3(I)

[a] The ratio of peak-to-valley yields of fission product mass distribution taken from von Gunten (ref. [3])) unless otherwise noted.

[b] B_N is experimental neutron binding energies calculated from the experimental masses tabulated by Myers and Swiatecki (ref. [22])).

[c] Compound nucleus excitation energy (E_T = incident neutron energy + neutron binding energy).

[d] E_i is the energy of the secondary minimum in the deformation energy surface relative to the ground state.

[e] E_a is the energy of the asymmetric second saddle point relative to the ground state.

[f] E_s is the energy of the symmetric second saddle point relative to the ground state.

[g] Nil-I - calculated values of h are taken from ref. [7]) (the case where surface dependent pairing strengths are used), and added to E_a to give E_s.

[h] Nil-II - calculated values of h are taken from ref. [7]) (the case where constant pairing strengths are used), and added to E_a to give E_s.

(continued)

Table 1 (continued)

[i] Pauli - calculated values of h are taken from ref. [16]) and added to E_a to give E_s.

[j] Nix - calculated values of h are taken from ref. [8]) and added to E_a to give E_s.

[k] Reference [16]).

[ℓ] Reference [13]).

[m] Reference [15]).

[n] Reference [14]).

[o] Reference [5]).

[p] Calculated value from ref. [22]).

[q] The value of h is estimated from deformation energy surface plots provided by Möller and Nilsson (ref. [7])).

[r] Reference [4]).

Table 2. Experimental and calculated values of peak-to-valley ratios for spontaneously fissioning nuclei[a].

Nucleus	Peak Yield/Valley Yield	
	Experimental	Calculated
^{238}U	> 500[b]	8×10^6
^{240}Pu	> 270[b]	7×10^5
^{242}Cm	> 700[b]	2.4×10^4
^{244}Cm	> 5×10^3 [c]	2×10^4
^{252}Cf	~ 750[b]	fitted
^{256}Fm	~ 12[c]	43

[a]Calculations were performed using eq. (5) with values of β and β' given by eq. (6a,b). Experimental parameters used in eq. (5) are presented in Table 1.

[b]Reference [3]).

[c]Reference [5]).

Figure Captions

Fig. 1. A typical mass yield curve. The data[2]) is presented for the neutron induced fission of ^{235}U at two neutron energies: thermal and 14 MeV.

Fig. 2. Schematic representation of a deformation energy surface as a function of symmetric and asymmetric deformations. For details see text.

Fig. 3. Classification of cases for study of mass asymmetry. Case I corresponds to the situation where the excitation energy E_T is above both the symmetric mountain top, E_s, and the asymmetric saddle point, E_a. Case II corresponds to the situation where E_T is above E_a, but below E_s. Case III corresponds to the situation where E_T is below both E_s and E_a.

Fig. 4. Correlation given by eq. (2) for Case I data using the Möller-Nilsson[7]) theoretical barriers. The line is drawn in to smoothly join experimental data points.

Fig. 5. Same as fig. 4 but using four sets of theoretical fission barriers: Δ → Möller and Nilsson[7]) using a surface dependent pairing strength (this is the same data used in fig. 4); + → Möller and Nilsson[7]) using a constant pairing strength; □ → Nix[8]); ● → Pauli and Ledergerber[16]). The two lines are drawn to bracket the experimental data.

Fig. 6. Correlation given by eq. (3) for Case I data. This graph is used for prediction of the (^{257}Fm, $n_{th}f$) peak-to-valley ratio. Möller and Nilsson's theoretical barriers are used.

Fig. 7. Correlation given by eq. (4) for Case II data using Möller and Nilsson theoretical barriers. The line is drawn through the experimental data points.

Fig. 8. Same as fig. 7 but using four sets of theoretical fission barriers: Δ - Möller and Nilsson[7]) with surface dependent pairing strength (this is the same data used in fig. 7), + - Möller and Nilsson[7]) with a constant pairing

strength, □ - Pauli and Ledergerber[16]), ● - Nix[8]). The lines are drawn joining the various sets of data.

Fig. 9. The dark line is a schematic representation of the fission barrier along symmetric deformations. The outer barrier is approximated by a parabola (dashed line) which passes through the secondary minimum and spontaneous fission emerging point and has the same maximum as the outer fission barrier. The penetration path (d) is from the second minimum to point of emergence. A similar approximation is applied for the asymmetric barrier.

Fig. 10. Deformation energy surface of ^{222}Ra in the region of the second saddle point as calculated by Möller and Nilsson[7]) using a constant pairing strength.

Fig. 11. A hypothetical representation of the triple peaked fission mass yields of nuclei in the radium region. The left-hand curve gives the cross-section of deformation energy surface near the outer peak as a function of shape asymmetry. The right-hand curves give the mass yields at various excitation energies indicated.

Fig. 12. A possible explanation of the experimentally observed mass yield distributions in the proton induced fission of ^{226}Ra. The mass yields of first (^{227}Ac) and second (^{226}Ac) chance fissions are indicated along with the cumulative fission mass yield. These yields are presented schematically for five different bombarding energies (E_p). The considerations of both the first and the second chance fission are necessary to explain the variation of the symmetric fission yield peak relative to the asymmetric yield peak.

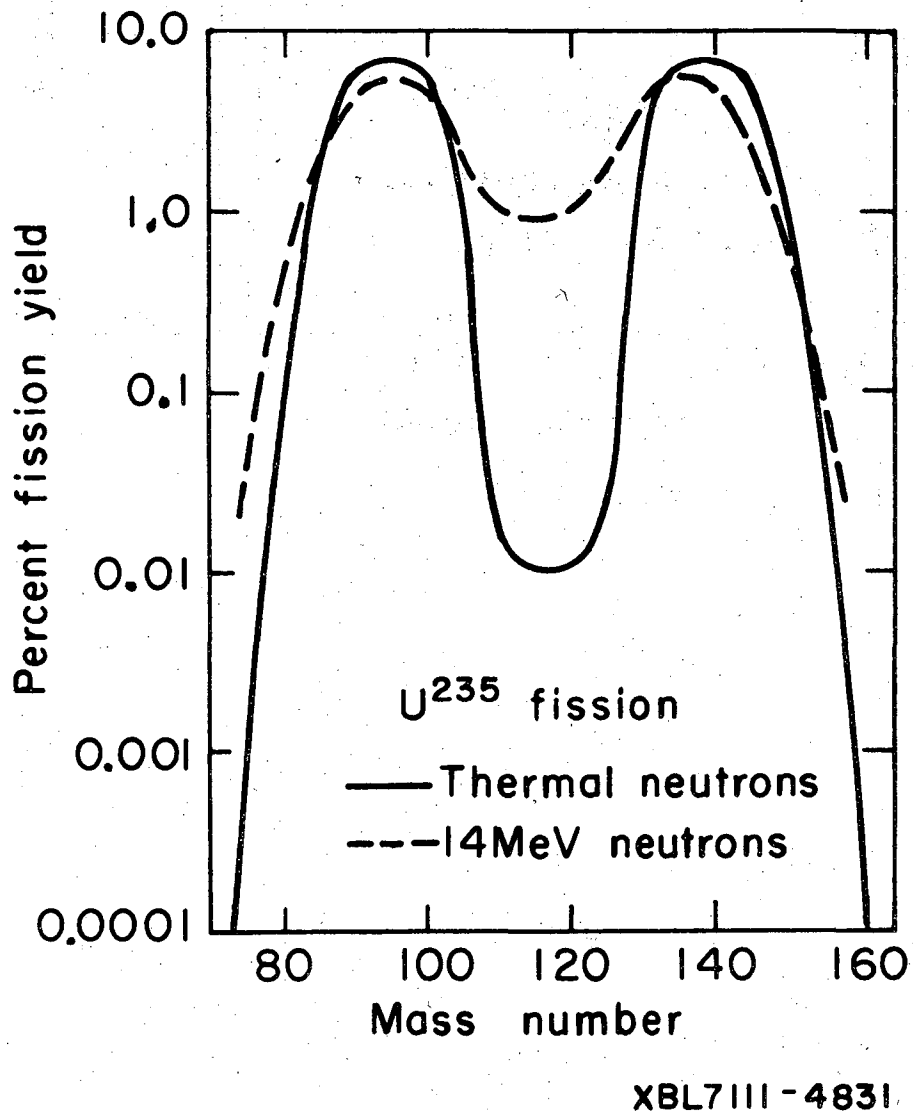
10.0
1.0
0.1
0.01
0.001
0.0001
Percent fission yield
80
100
120
140
160
Mass number
U235 fission
Thermal neutrons
14MeV neutrons
XBL7111-4831

Fig. 1

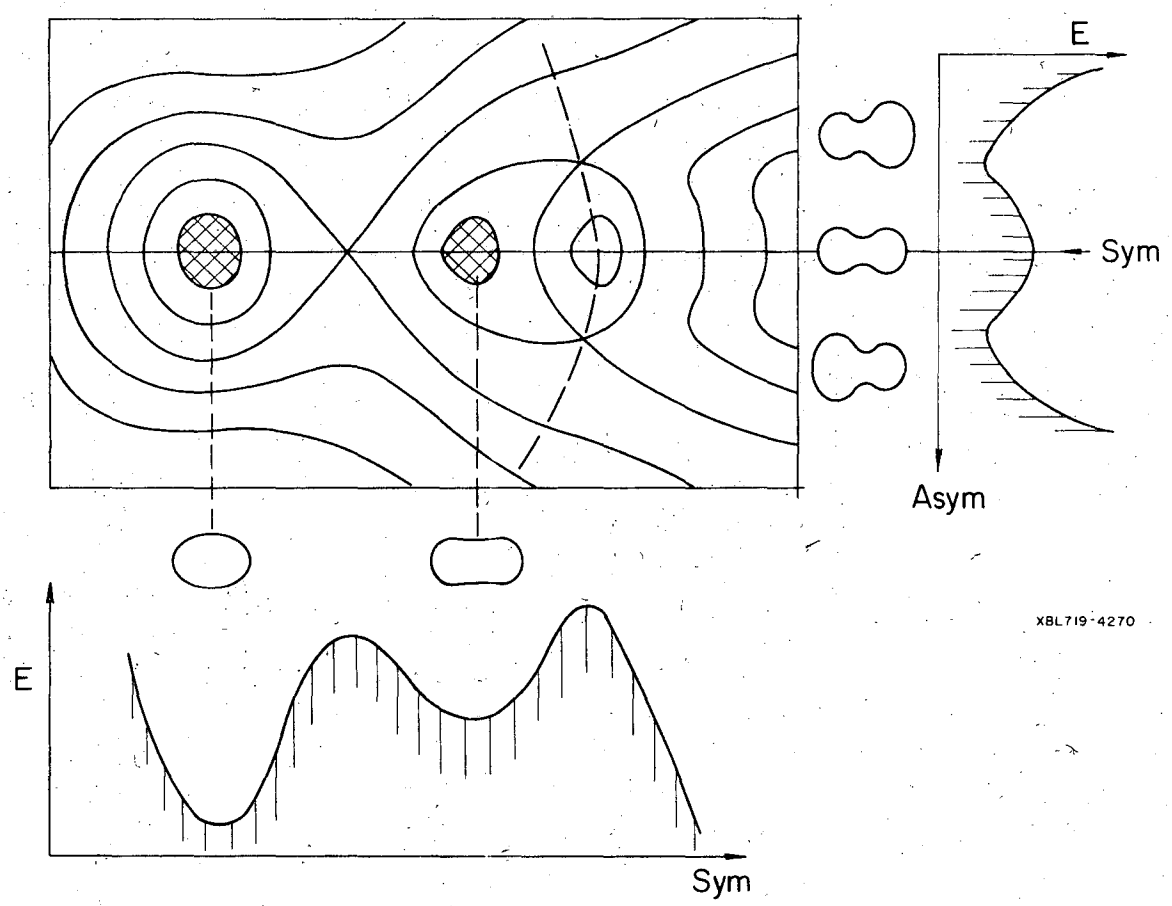

Fig. 2

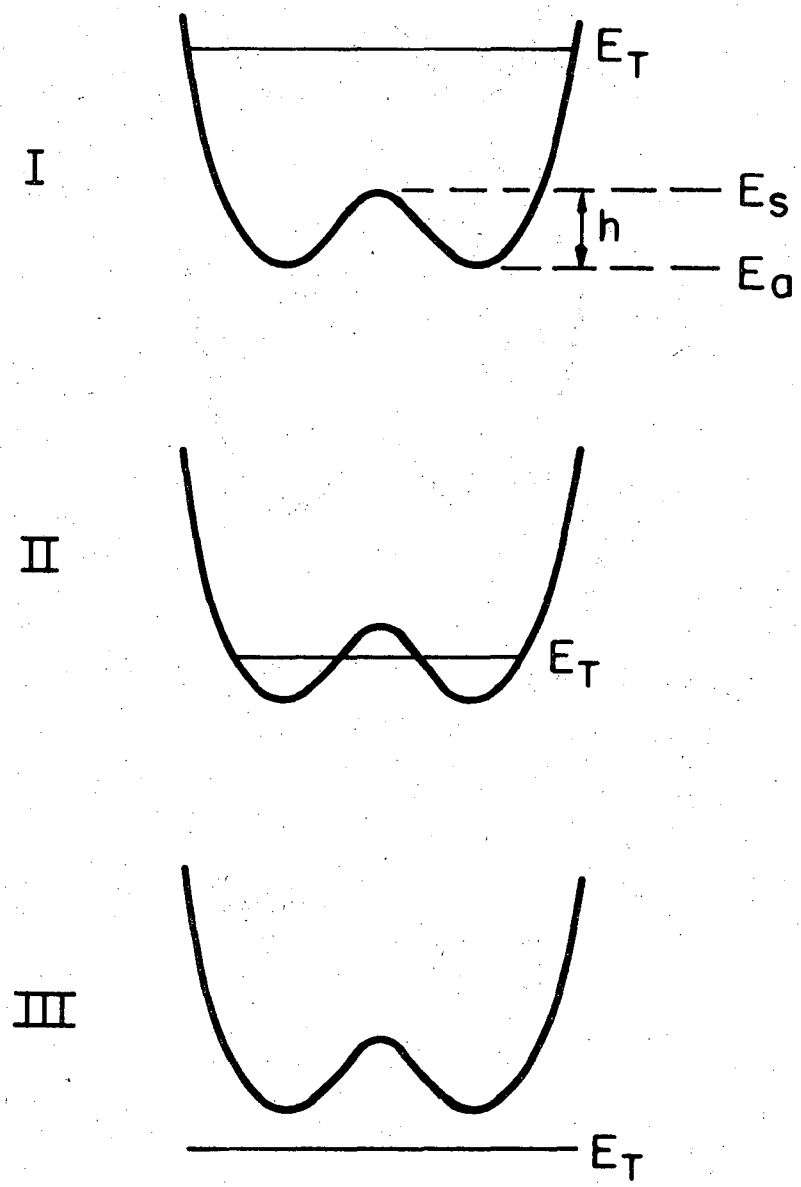

XBL7111-4829

Fig. 3

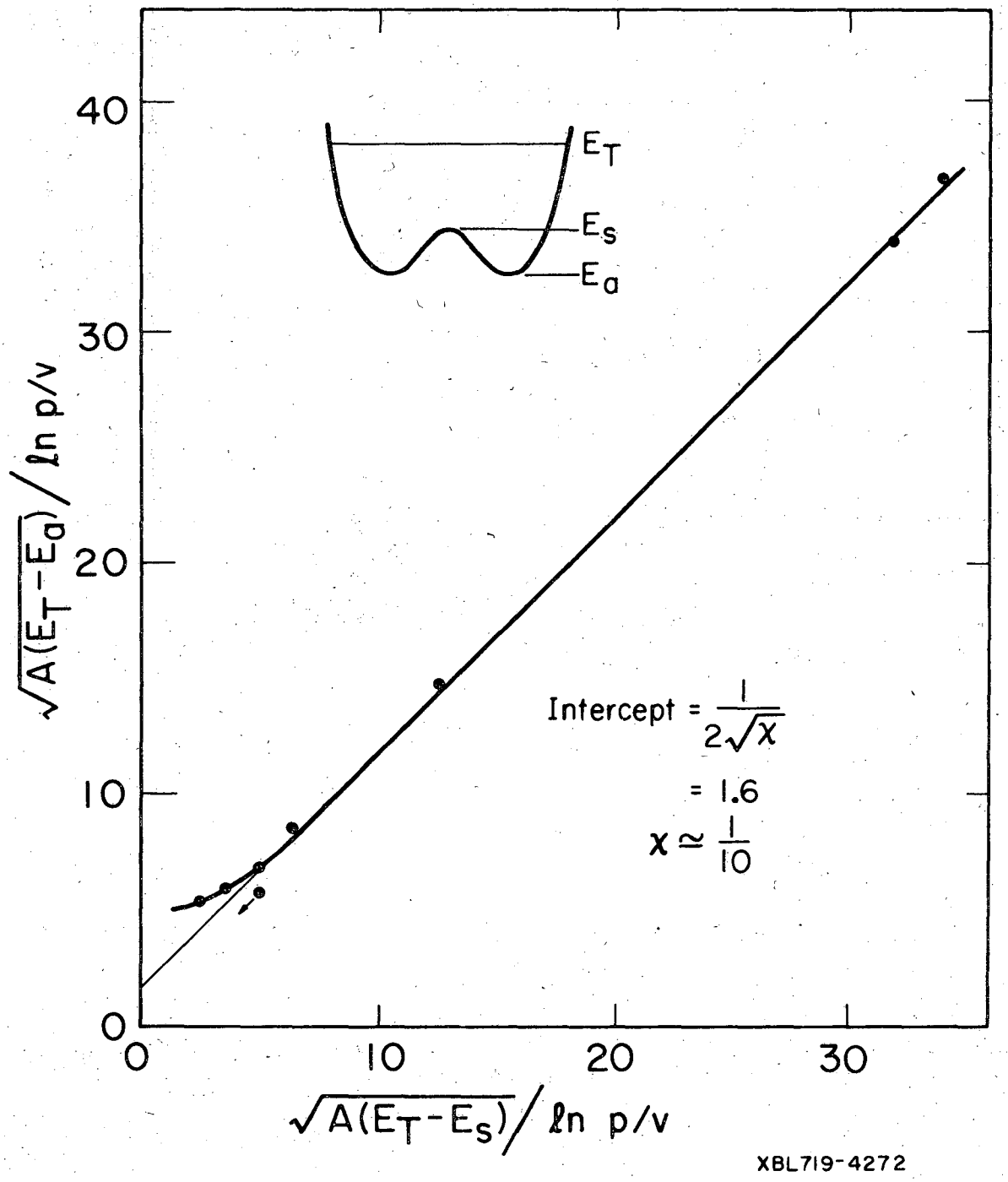
40
30
20
10
0
0
10
20
30
$\sqrt{A(E_T-E_a)}/\ln p/v$
$\sqrt{A(E_T-E_s)}/\ln p/v$
E_T
E_s
E_a
Intercept = $\frac{1}{2\sqrt{x}}$
= 1.6
$x \simeq \frac{1}{10}$
XBL719-4272

Fig. 4

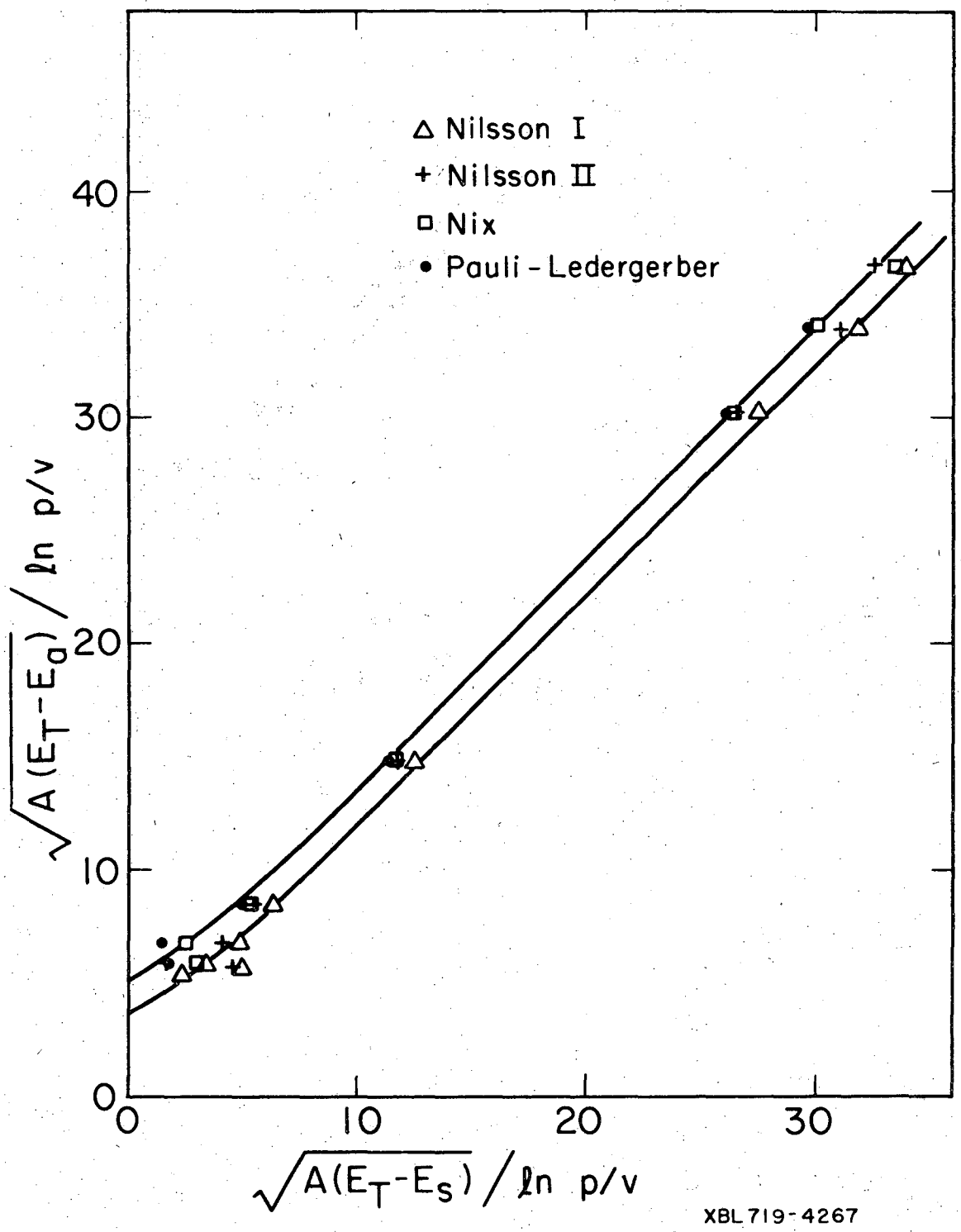
△ Nilsson I
+ Nilsson II
□ Nix
• Pauli - Ledergerber
40
30
20
10
0
0
10
20
30
$\sqrt{A(E_T-E_a)}$ / ln p/v
$\sqrt{A(E_T-E_s)}$ / ln p/v
XBL 719-4267

Fig. 5

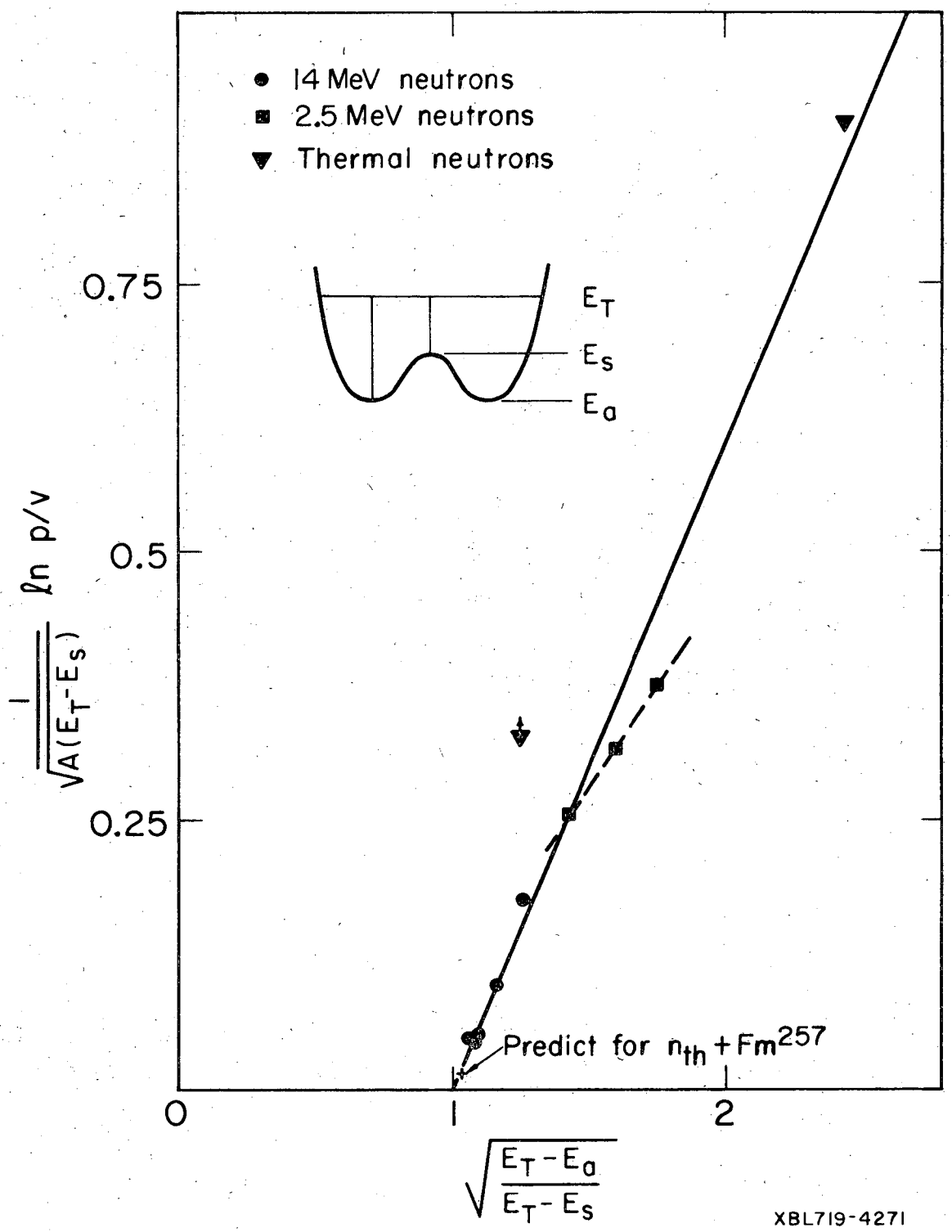
14 MeV neutrons
2.5 MeV neutrons
Thermal neutrons
E_T
E_s
E_a
0.75
0.5
0.25
$\frac{1}{\sqrt{A(E_T-E_s)}} \ln p/v$
Predict for $n_{th} + Fm^{257}$
0
1
2
$\sqrt{\frac{E_T-E_a}{E_T-E_s}}$
XBL719-4271

Fig. 6

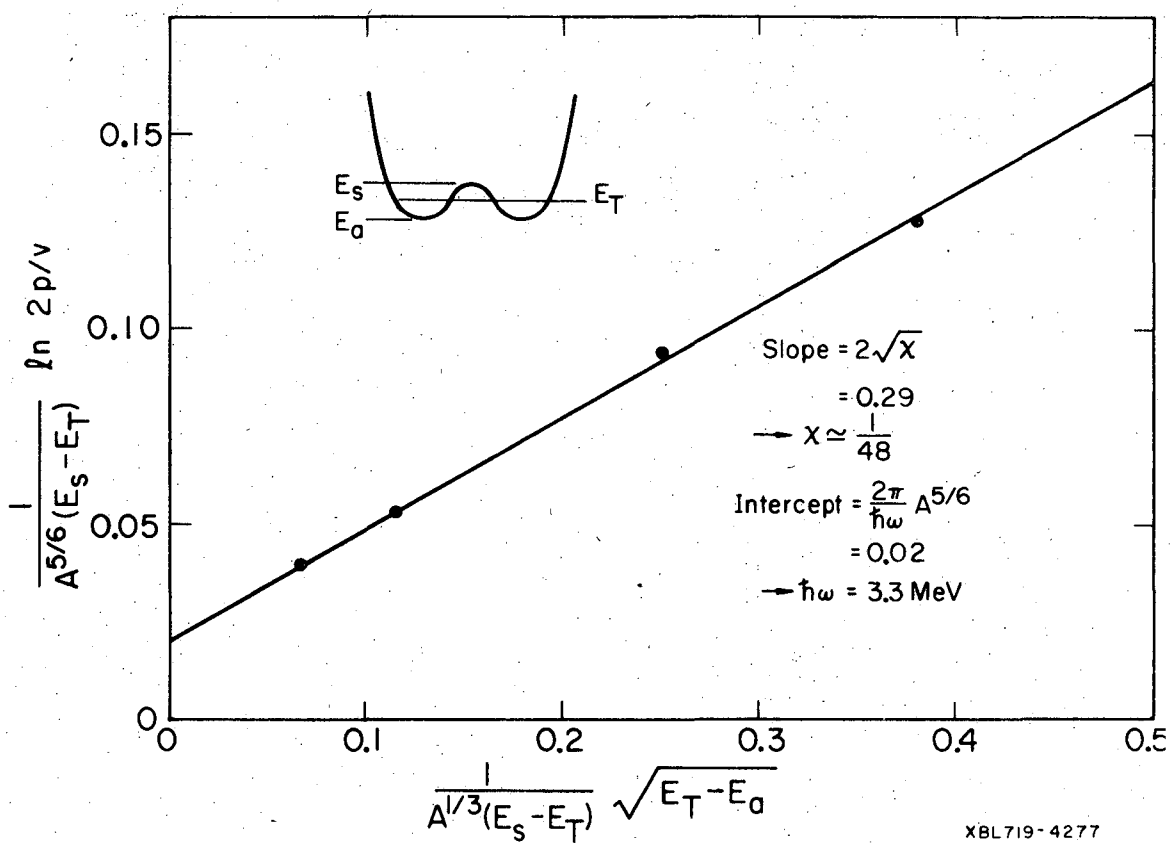
0.15
0.10
0.05
0
0
0.1
0.2
0.3
0.4
0.5
$\frac{1}{A^{5/6}(E_s-E_T)} \ln 2p/v$
$\frac{1}{A^{1/3}(E_s-E_T)} \sqrt{E_T-E_a}$
E_s
E_a
E_T
Slope = $2\sqrt{x}$
= 0.29
$\rightarrow x \simeq \frac{1}{48}$
Intercept = $\frac{2\pi}{\hbar\omega} A^{5/6}$
= 0.02
$\rightarrow \hbar\omega$ = 3.3 MeV
XBL719-4277

Fig. 7

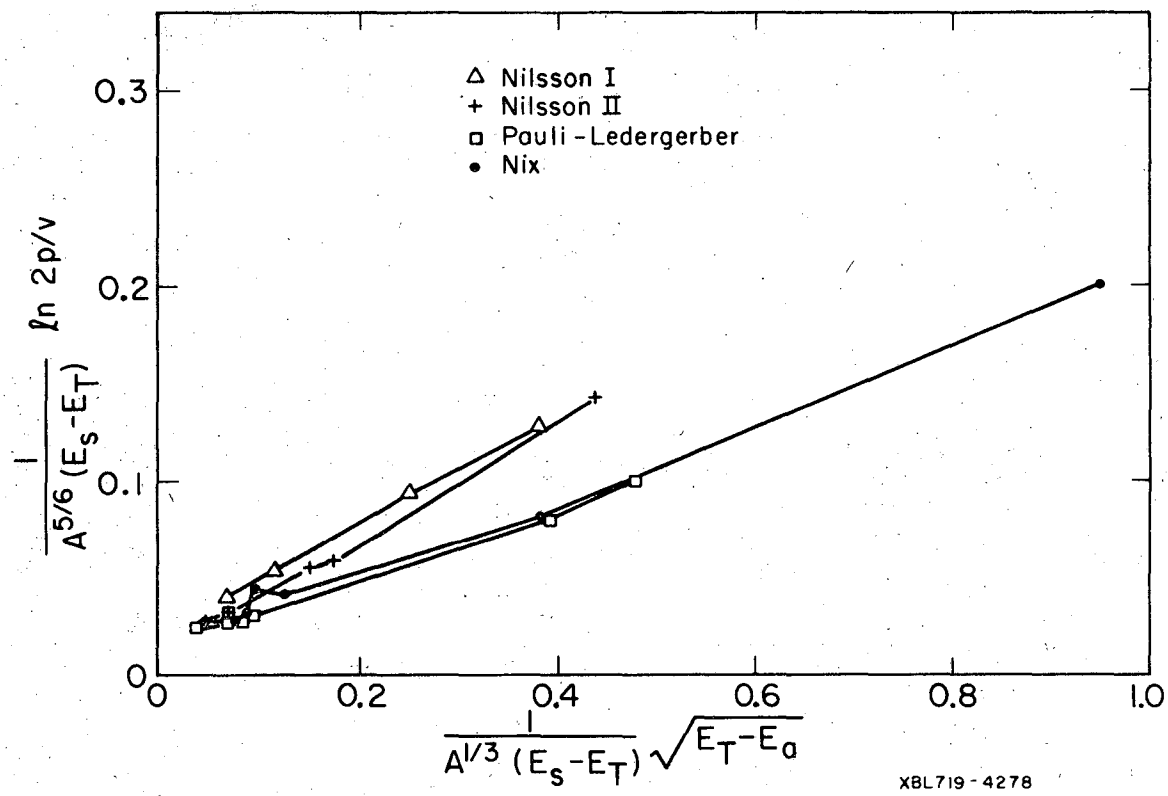
Nilsson I
Nilsson II
Pauli-Ledergerber
Nix
0.3
0.2
0.1
0
0
0.2
0.4
0.6
0.8
1.0
$\frac{1}{A^{5/6}(E_s-E_T)} \ln 2p/v$
$\frac{1}{A^{1/3}(E_s-E_T)}\sqrt{E_T-E_a}$
XBL719-4278

Fig. 8

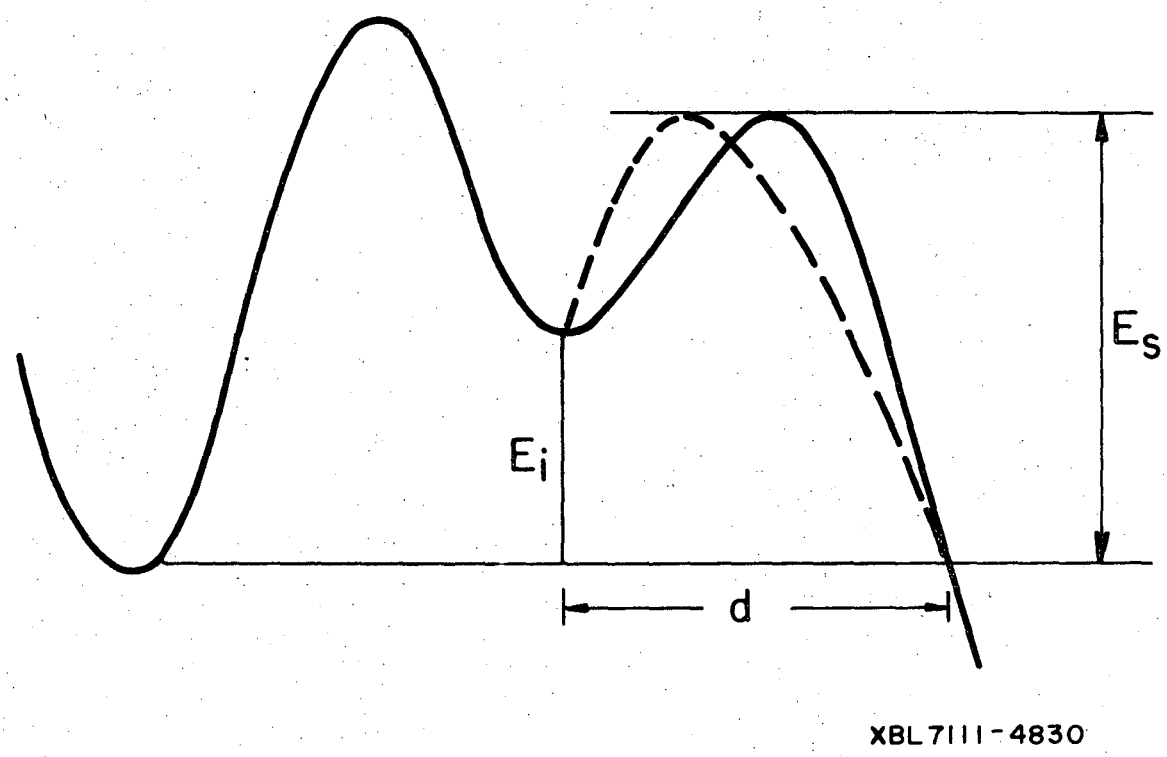

Fig. 9

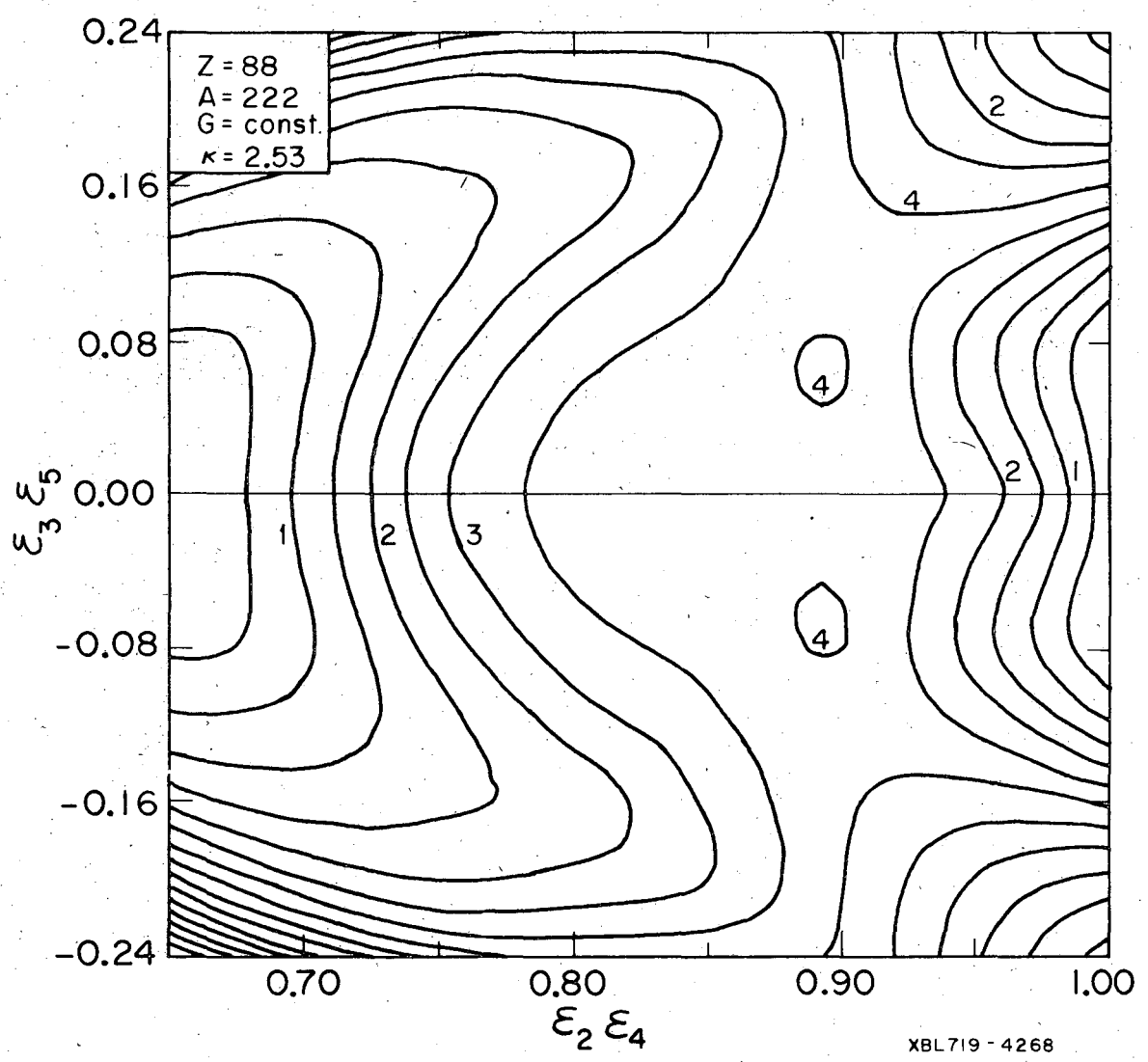
Z = 88
A = 222
G = const.
κ = 2.53
0.24
0.16
0.08
0.00
-0.08
-0.16
-0.24
0.70
0.80
0.90
1.00
ε3 ε5
ε2 ε4
1
2
3
4
XBL719-4268

Fig. 10

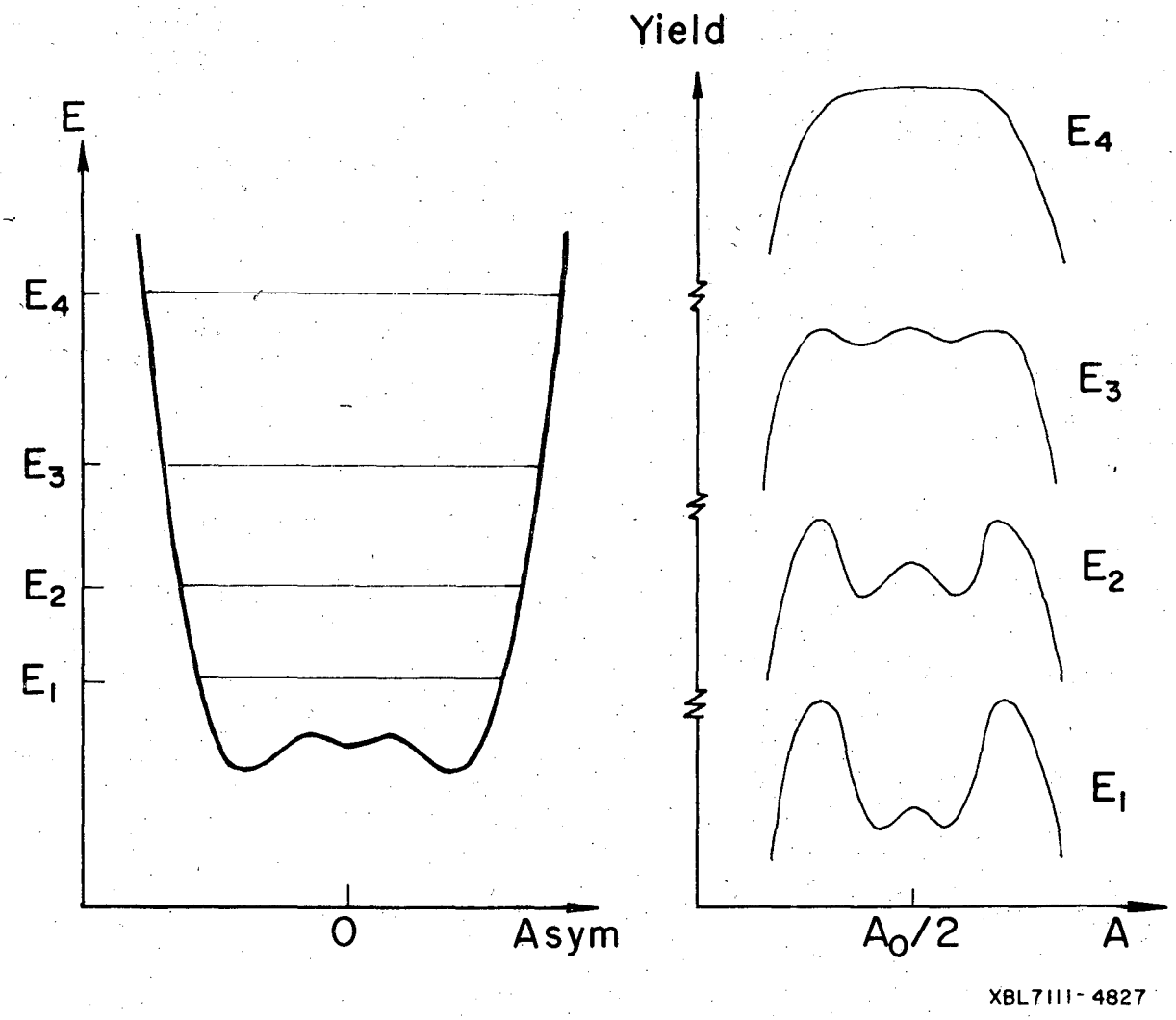

Fig. 11

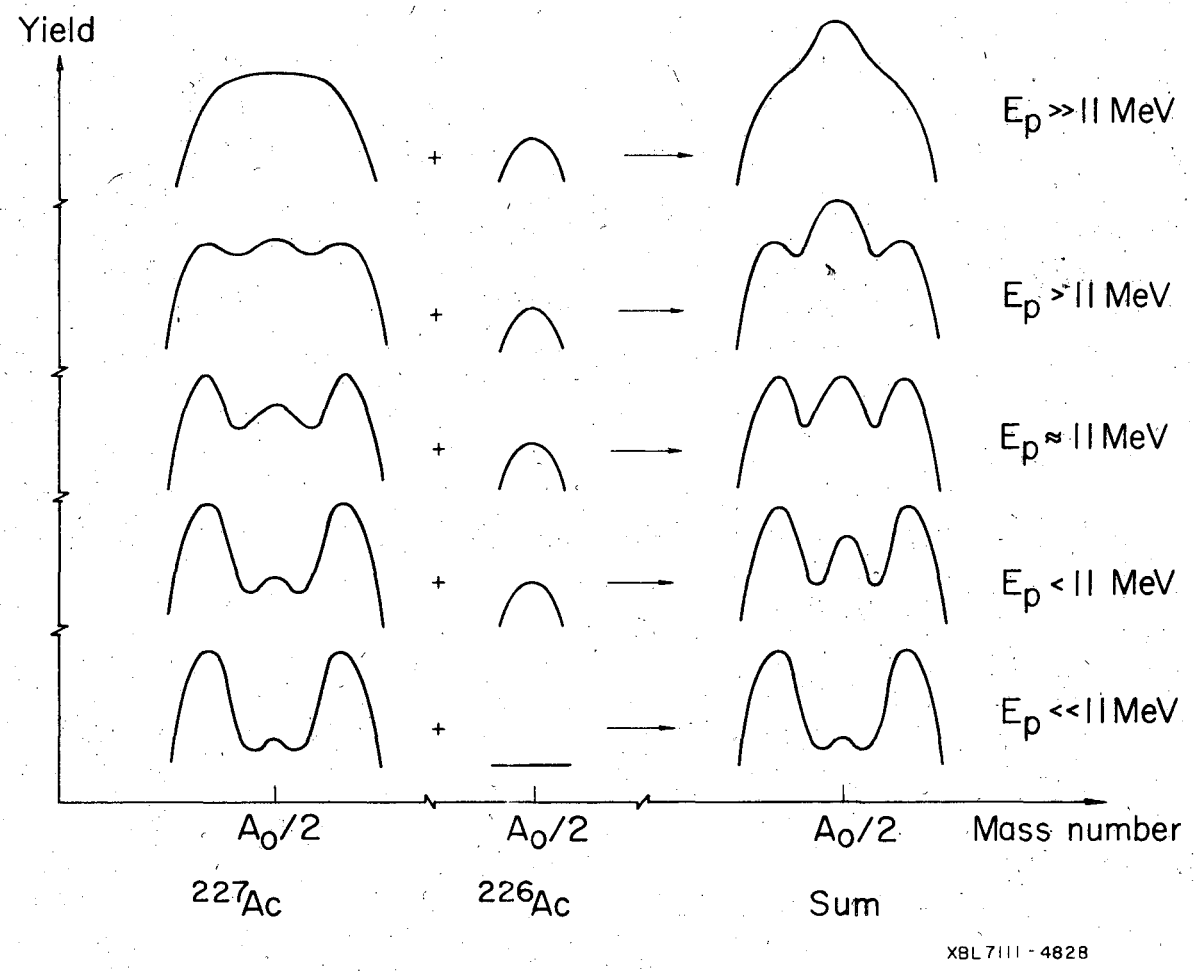
Yield
$E_p \gg 11$ MeV
$E_p > 11$ MeV
$E_p \approx 11$ MeV
$E_p < 11$ MeV
$E_p \ll 11$ MeV
$A_0/2$
$A_0/2$
$A_0/2$
Mass number
^{227}Ac
^{226}Ac
Sum
XBL 7111-4828

Fig. 12

LEGAL NOTICE

This report was prepared as an account of work sponsored by the United States Government. Neither the United States nor the United States Atomic Energy Commission, nor any of their employees, nor any of their contractors, subcontractors, or their employees, makes any warranty, express or implied, or assumes any legal liability or responsibility for the accuracy, completeness or usefulness of any information, apparatus, product or process disclosed, or represents that its use would not infringe privately owned rights.

TECHNICAL INFORMATION DIVISION
LAWRENCE BERKELEY LABORATORY
UNIVERSITY OF CALIFORNIA
BERKELEY, CALIFORNIA 94720